Available online at www.sciencedirect.com
SCIENCE DIRECT®
Acta Materialia 52 (2004) 2429–2434
Acta MATERIALIA
www.actamat-journals.com

Shear band spacing under bending of Zr-based metallic glass plates

R.D. Conner [a,*], Yi Li [b], W.D. Nix [c], W.L. Johnson [a]

[a] Keck laboratory, Department of Materials Science, California Institute of Technology, Mail Stop 138-78, Pasadena, CA 91125, USA
[b] Department of Materials Science, National University of Singapore, Singapore 119260, Singapore
[c] Department of Materials Science and Engineering, Stanford University, Stanford, CA 94305-2205, USA

Received 26 September 2003; received in revised form 23 January 2004; accepted 27 January 2004

Abstract

Metallic glasses often exhibit marked ductility when subjected to compressive or bending loads as a result of multiple shear band formation. This observed ductility depends upon sample geometry; thin plates show ductility in bending while thicker plates of the same composition fracture under similar loading. The thickness dependence of yielding and fracture of metallic glass plates subjected to bending is considered in terms of the shear band processes responsible for these properties. Experimental results show that shear band spacing and length scale with the thickness of the plate at a ratio of 1:10. Both shear band offset and shear band spacing increase with increasing curvature; shear band offset as the square of the plate thickness. As bending is increased beyond yield, shear band spacing continues to increase until the strain is accommodated by a few long shear bands. Continued bending leads to crack formation and failure.

Keywords: Metallic glasses; Bending test; Ductility; Shear bands

1. Introduction

Experimental evidence has shown that metallic glasses undergo permanent deformation through the generation of shear bands. Whether these materials experience plastic deformation depends upon sample geometry and testing procedure. For example, under compressive loading, samples with small aspect ratios (<1.5:1) can deform in an elastic-perfectly plastic manner, while those with aspect ratios in excess of 1.5:1 show little, if any, plastic deformation, and bulk metallic glass rods loaded in uniaxial tension invariably fail by the propagation of a single shear band. Similarly, thin wires or ribbons of metallic glass bend without failure, but thicker plates fail catastrophically under bending. Plastic deformation is accommodated through the generation of multiple shear bands. Shear bands can be constrained in compression samples with low aspect ratio and metallic glass composites. Bending is an inherently stable method of deformation, as the stress to drive shear bands diminishes as the shear band approaches the neutral axis. In 1980, Ast and Krenitsky [1] illustrated how thin (~50 μm) Fe40Ni40P14B6 metallic glass ribbons deform as an ideal elastic–plastic solid, and Zielinski and Ast [2] subsequently showed that Ni–Si–B wires formed multiple shear bands in bending. Many additional reports can be found in the literature of thin wires or foils of amorphous metals having good ductility in bending [3–9]. Katuya et al. [10] and Inoue et al. [11,12] found that significant bend ductility may be achieved only if the sample dimension is below a critical value, suggesting a size effect for bend ductility.

The observation that thin wires of metallic glasses can be bent plastically while thick plates do not is not expected for elastic, perfectly-plastic materials subjected to bending since this mode of deformation is inherently stable. Metallic glasses, with compressive deformation properties showing elastic, perfectly-plastic behavior, might be expected to deform stably in bending regardless of the plate thickness, yet thick plates of metallic glasses invariably fracture in bending while thin ribbons deform extensively. We wish to understand this sample

* Corresponding author. Tel.: +1-626-395-4425; fax: +1-626-795-6132.
E-mail address: rdconner@caltech.edu (R.D. Conner).

1359-6454/$30.00 © 2004 Acta Materialia Inc. Published by Elsevier Ltd. All rights reserved.
doi:10.1016/j.actamat.2004.01.034

size effect, as it could be of importance in the development of ductile metallic glass alloys.

Shear band formation, organization, and spacing has been investigated by a number of reseachers, particularly with respect to dynamic deformation. Li addressed the behavior and properties of shear bands in polymers [13], and later extended the concepts to amorphous alloys [14]. Grady [15] proposed that shear band spacing is related to the wavelength of perturbations that develop in initially homogeneous materials, with areas of deformation localized by momentum diffusion. Wright and Ockendon [16,17] extended the perturbation concept to include materials with strain rate sensitivity, followed by Molinari [18], who modified the W–O theory to include strain hardening. Nesterenko et al. [19] used these models to analyze shear band spacing formed during dynamic deformation of titanium; these experiments were extended by Xue et al. [20] in comparison of shear band spacing of Ti and Ti–6Al–4V alloys.

The present work examines the effect of sample thickness and bend radius on the bending ductility of $Zr_{57}Nb_5Al_{10}Cu_{15.4}Ni_{12.6}$ bulk metallic glass. The properties of $Zr_{57}Nb_5Al_{10}Cu_{15.4}Ni_{12.6}$ are listed in Table 1. It demonstrates that the plastic strain to failure for metallic glass wires and foils increases with decreasing sample dimension. By bending wires and strips of varying thickness around mandrels of different radii we find that the strain to fracture increases markedly as the sample thickness drops below about 1 mm, and that the shear band spacing on the surface of the bent wires scales linearly with the sample dimension, as shown in Fig. 2. There, the shear band spacing is observed to be about one tenth of the sample thickness over a wide range of sample sizes. Both shear band offset and shear band spacing increase with increasing curvature. Shear band offset at given curvature increases as the square of the plate thickness. These are important sample size effects which, we believe, leads to the strong effect of sample size on bend ductility.

Table 1
Mechanical and physical properties of $Zr_{57}Nb_5Al_{10}Cu_{15.4}Ni_{12.6}$ (Vitreloy 106)

Property	$Zr_{57}Nb_5Al_{10}Cu_{15.4}Ni_{12.6}$
CTE (10^{-6} μm m^{-1} °C^{-1})	8.7
Elastic modulus (GPa)	86.7
Poisson's ratio (v)	0.38
Density (g cm^3)	6.8
Bulk modulus (GPa)	118
Shear modulus (GPa)	30.8
Ultimate strength (MPa)	1800[a]
	1200[b]
Yield strength (MPa)	1800[a]
	1200[b]
Elongation (%)	2

[a] Uniaxial compression.
[b] Uniaxial tension.

2. Experimental method

Ingots of $Zr_{57}Cu_{15.4}Ni_{12.6}Al_{10}Nb_5$ (at.%) bulk metallic glass (BMG) were made by arc melting and mixing elemental metals (>99.9% purity, metals basis) on a water-cooled copper hearth in a titanium-gettered argon atmosphere. The amorphous ingots were induction melted and cast into a copper mold in an argon-purged vacuum furnace. The cast ingots had dimensions 4 mm × 6 mm × 35 mm. These ingots were then sliced into thin (0.28 mm $< t <$ 1.46 mm) BMG plates using a diamond saw. Burrs from the cutting process were removed by lapping on SiC paper. The BMG plates were clamped in a sheet-metal bending brake and bent around dies with radii of 0.5, 1, 2 and 3 mm.

Thin BMG ribbons 50 and 86-μm thick were made on a melt spinner having a tangential velocity of 40 and 35 m/s, respectively. The ribbons were bent around a razor blade to form a right angle.

The bent plates and ribbons were examined using scanning electron microscopy (SEM). Shear band spacing and offset were measured by averaging the number of shear bands over the sample length, or averaging the offset height.

3. Results

Microscopic analysis reveals that a multiplicity of shear bands form when the sample is bent. As depicted in Fig. 1, primary shear bands form at both the inside (compression) and outside (tension) surfaces of the sample. The shear bands on both surfaces show uniform initial spacing, shear steps (offset) with respect to their neighbors, and initially propagate at ~50° with respect to the free surface. Those on the tensile side tend to be longer and more uniformly spaced than those on the compression side, and reveal a regular slip offset with respect to the sample surface. The shear bands in Fig. 1(a) all bend in the same direction (''left''), while those in Fig. 1(b) bend to the ''left'' and to the ''right''. Xue found left and right behavior in Ti and Ti–6Al–4V under dynamic deformation [20]; however, in the present case, the change in direction is likely due to the constraints imposed by the bending brake, bending the metallic glass strip around a mandrel. On the tensile side, secondary shear bands form along the length of the primary shear bands, particularly below the area of the shear offset, and tertiary shear bands form within the secondary shear bands. Primary shear bands that form on the compression side do not penetrate to uniform thickness or form at consistent angles with respect to the sample surface. Secondary and tertiary shear bands on the compression side form numerous branches but do not generate the evenly spaced secondary and tertiary shear bands found on the tensile side. These shear bands

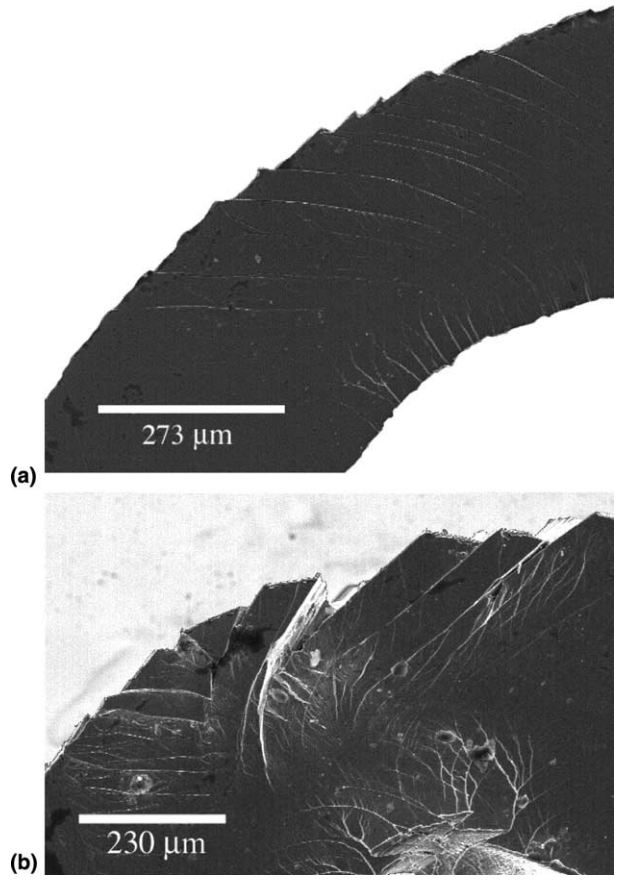

Fig. 1. (a) 0.457 mm-thick sample bent around a 2-mm radius; (b) a 0.584-mm thick sample bent around a 2 mm radius. Note that the shear band spacing in (a) is much finer than in (b) and that the shear steps show less offset. In (b), the shear band propagates to the neutral axis and a critical crack has formed; also, there are numerous secondary shear bands on the tensile side, and many more shear band bifurcations on the compression side.

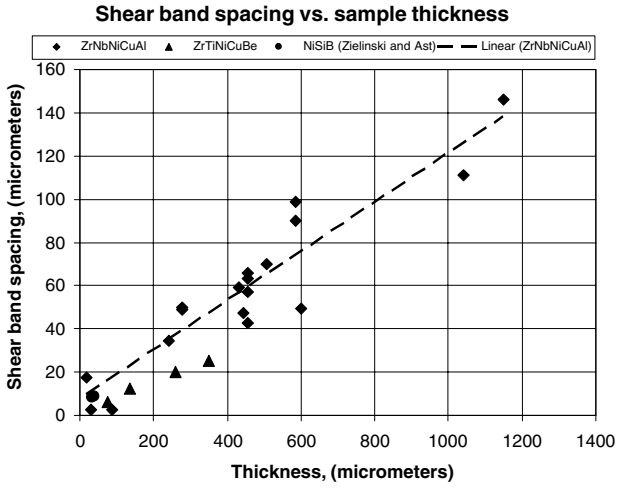

Fig. 2. Shear band spacing versus sample thickness measured on the tensile (outside) of the bend. Note the strong correlation between sample thickness and shear band spacing.

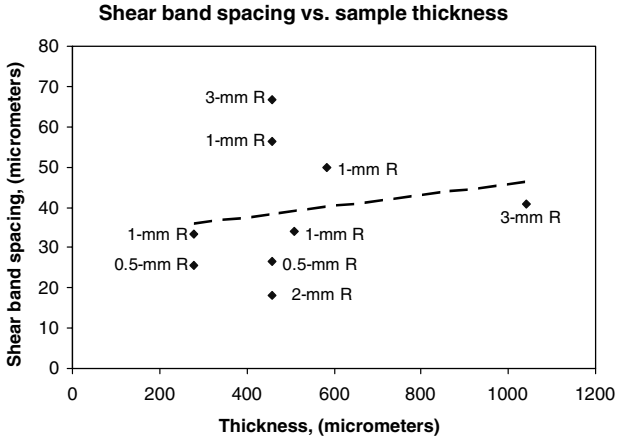

Fig. 3. Shear band spacing on the compression (inside) of the bend. Data points are labeled according to bend radius. Note that there is still a relationship between specimen thickness and shear band spacing.

appear similar to those found by Xue. Note that the radius of curvature of the shear bands decreases moving toward the center of the sample, and that more secondary shear bands are generated as the bend radius becomes more severe.

The shear band spacing is plotted as a function of sample thickness in Fig. 2 and Fig. 3, for outside and inside bend radius, respectively. Fig. 2 shows that shear band spacing increases with sample thickness with a slope of 1:10. This graph includes results from Zr–Ti–Ni–Cu–Be and Ni–Si–B metallic glass alloys, and shows consistent results regardless of glassy alloy tested. Fig. 3 plots shear band spacing versus thickness and also with respect to the bend radius of the mandrel on the compression side of the sample. These compression shear bands show a similar increase in spacing with sample thickness though the increase is not as pronounced. The change in shear band spacing with bend radius does not vary in a uniform or predictable way under compression.

The spacing between secondary shear bands increases with increasing thickness of the primary shear band just as primary shear band spacing increases with increasing plate thickness (Fig. 4). Although the spacing is not quite as uniform and the method of averaging measurements tends to increase scatter in the results, Fig. 4 still shows that secondary shear band spacing increases with increasing primary shear band thickness at a ratio of about 1:5.

In addition to the spacing of primary and secondary shear bands with respect to thickness, there is a strong correlation between the shear offset with both the sample thickness and the bend radius.

Fig. 5(a) shows the shear band offset versus sample thickness, for samples bent around a 1 mm mandrel. The shear band offset increases as an apparently parabolic function of sample thickness at constant bend

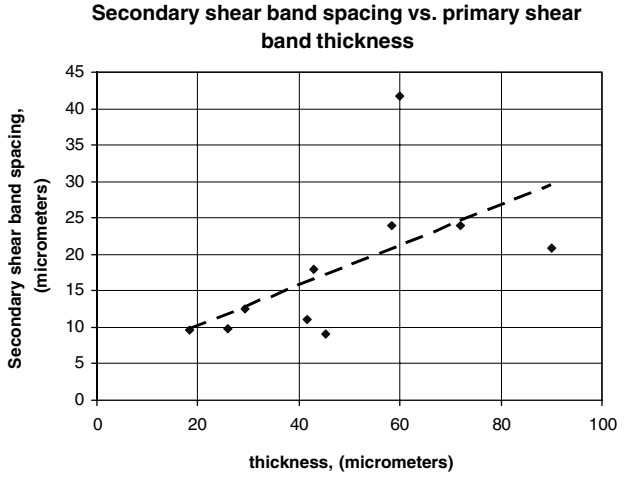

Fig. 4. Secondary shear band spacing as a function of sample thickness and primary shear band thickness.

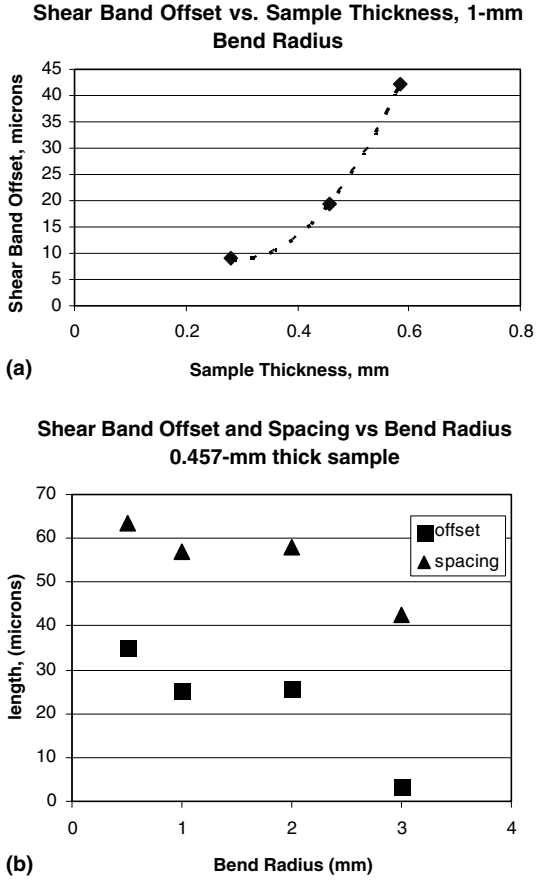

Fig. 5. (a) Shear band offset versus sample thickness, for given bend radii. (b) Shear band offset versus bend radius for a constant sample thickness.

radius. Fig. 5(b) plots shear band offset and shear band spacing as a function of bend radius for samples of constant (0.457 mm) thickness. The bend radii are 0.5, 1, 2 and 3 mm. This figure reveals that shear band spacing and shear band offset steadily decrease with increasing bend radius for constant sample thickness.

Secondary shear band spacing as a function of bend radius was measured. The bend radius was estimated by drawing lines perpendicular to the bend section at each end, then measuring the radius from the point at which the lines intersect. The results show that secondary shear band spacing for a given primary shear band thickness varies little with respect to the curvature. This is contrary to visual observation of shear bands in Fig. 1, in which secondary shear bands appear to cluster in the areas in which the primary shear bands are tightly bent. It also contradicts the results reported above for primary shear bands and disagrees with the theoretical development below. This may result from both averaging over the spacing of large numbers of primary and secondary shear bands and the imprecision of estimating the radius of curvature in the primary shear bands.

4. Discussion

Referring to the development for shear band spacing in metallic glasses by Conner et al. [21], we see that shear band spacing in bending is expected to scale with the thickness of a plate:

$$\lambda = \frac{(1-2\nu)}{(1-\nu)}\left(1-\frac{\kappa_y}{\kappa}\right)^2 h, \tag{1}$$

where λ is the shear band spacing, ν is Poisson's ratio, the curvature $\kappa = 1/R_n$, the bend radius at the neutral axis, κ_y is the curvature at the yield surface, and h is the distance from the neutral axis or centroid of the plate. The geometry for symmetric plane strain bending and shear band spacing is depicted in Fig. 6. Graphing shear band spacing versus sample thickness shows that this kind of relation is very well obeyed for various metallic glasses, particularly for primary (Fig. 2) and secondary shear bands (Fig. 4) on the tensile side of the bend specimen. The slope in Fig. 2 is ~1:10, while that in Fig. 4 is ~1:5. This agreement is remarkable considering the constraint the surrounding material applies to the secondary shear bands which is absent on the primary shear bands.

The results from the side under compression, Fig. 3, follow the same trend, though the results are not as convincing. The secondary shear bands tend to form in clusters of branches initiating at points along the primary shear bands very close to the sample surface. This results because the material is in a highly constrained state of compressive stress. Metallic glass samples with aspect ratios less than 1.5 has been shown to behave in an elastic-perfectly plastic manner when loaded in compression, resulting from geometrical constraints on shear band propagation [22]. Eq. (1) also indicates that the shear band spacing should increase with increasing

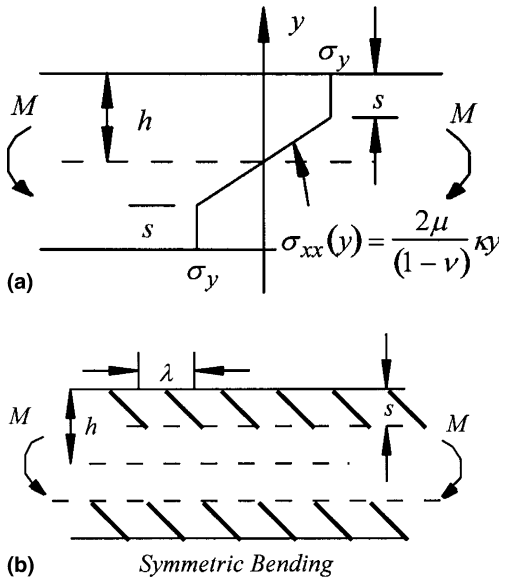

Fig. 6. (a) Stress distribution in a plate under plane strain *symmetric bending*. (b) Shear bands in a bent plate.

curvature (decreasing bend radius), but the results shown in Fig. 4 do not follow this trend.

From [21] we see that shear band spacing is related to the shear band offset at the tensile surface by:

$$\lambda = \frac{\Delta u_{\max}}{\sqrt{2}\varepsilon_{xx}(y=h)}, \tag{2}$$

in which $\Delta u_{\max}$ = shear band offset and ε_{xx} is the strain in the x direction. By substituting the equation for strain:

$$\varepsilon_{xx} = \kappa(y - y_0) \tag{3}$$

(at $y = h$, $y_0 = 0$) into Eq. (2) and equating this with the RHS of Eq. (1), we get an expression of maximum offset as a function of curvature and sample thickness

$$\Delta u_{\max} = \sqrt{2}\left(\frac{1-2\nu}{1-\nu}\right)\kappa\left(1 - \frac{\kappa_y}{\kappa}\right)^2 h^2. \tag{4}$$

From this equation and Eq. (1), we can see that as the bend radius decreases (curvature increases) for constant thickness samples, that both the shear band offset and shear band spacing increase. Also, Eq. (4) shows that offset increases as the sample thickness squared at constant κ. These experimental measurements are plotted in Fig. 5, in which it can be seen that this is the case.

Eq. 1 shows that shear band spacing is zero at the point of yielding ($\kappa = \kappa_y$), and increases with increasing curvature. Increasing sample thickness increases both shear band spacing and shear band length. As bending continues, a few widely spaced shear bands rapidly approach the neutral axis, at which stresses diminish and they no longer slip. Shear band propagation along the widely spaced bands relieves the shear stress on the intermediate bands. Similar stress shielding effects are reported by Xue [20] in Ti alloys. The slip along a few widely spaced shear bands causes a dramatic increase in the slip offset, eventually leading to crack nucleation. As may be seen from Fig. 1(b), the longest shear band has opened as a crack at the sample surface. This occurs because when the shear band reaches the neutral axis and the stress drops to zero, the remaining material on the compression side of the sample acts as a plastic hinge, opening the crack. Increasing sample thickness or decreasing bend radius both serve to increase the strain at the outer fibers of the sample. A crack forms when the strain can no longer be accommodated by the generation of many shear bands. Further bending leads to catastrophic failure.

5. Conclusions

This work shows that shear band spacing in metallic glass plates in bending varies linearly with plate thickness, at a ratio of ~1:10. Both shear band offset and shear band spacing increase with increasing curvature, as the square of the plate thickness. As bending is increased beyond yield, shear band spacing continues to increase until the strain is accommodated by a few long shear bands. Continued bending leads to crack formation and failure.

Acknowledgements

The authors gratefully acknowledge financial support for this work from the Defense Advanced Research Projects Agency (DARPA), under ARO Contract No. DAAD 19-01-1-525, and Dr. Leo Christodoulou as Program Manager.

References

[1] Ast DG, Krenitsky DJ. Evidence for ideal elastic–plastic deformation in Fe–Ni based metallic glasses. Mater Sci Eng 1980;43:241–6.
[2] Zielinski PG, Ast DG. Slip bands in metallic glasses. Phil Mag A 1983;48(5):811–24.
[3] Petouhoff NL, Ardell AJ, Jankowski AF. Mechanical behavior of both sides of an amorphous Fe78B14S18 alloy ribbon as determined from miniaturized disk-bend tests. Acta Metal Mater 1992;40(11):3167–77.
[4] Suto S, Matsuno K, Sano T, Matsui K. Bending of amorphous alloys. J Mater Proc Technol 1992;33(3):215–27.
[5] Inoue A, Amiya K, Yoshi I, Kimura HM, Masumoto T. Production of Al-based amorphous alloy wires with high tensile strength by melt extraction method. Mater Trans JIM 1994;35(7):485–8.
[6] Inoue A, Amiya K, Katsuya A, Masumoto T. Mechanical properties and thermal stability of Ti-based and Al-based amorphous wires prepared by a melt extraction method. Mater Trans JIM 1995;36(7):858–65.

[7] Barth EP, Spaepen F, Bye R, Das SK. Influence of processing on the ductile-to-brittle transition temperature of an Fe–B–Si metallic glass. Acta Mater 1997;45(1):423–8.
[8] Katsuya A, Inoue A, Masumoto T. Production and properties of amorphous alloy wires in Fe–B based system by a melt extraction method. Mater Sci Eng A – Struct Mater: Prop Microstruct Process 1997;226:104–7.
[9] Inoue A, Wang XM. Bulk amorphous FC20 (Fe–C–Xi) alloys with small amounts of B and their crystallized structure and mechanical properties. Acta Mater 2000;48(6):1383–95.
[10] Yokoyama Y, Yamano K, Fukaura K, Sunada H, Inoue A. Enhancement of ductility and plasticity of Zr55Cu30Al10Ni5 bulk glassy alloy by cold rolling. Mater Trans JIM 2001;42(4): 623–32.
[11] Katuya A, Inoue A, Amiya K. Production of Ni–Si–B amorphous alloy wires by melt extraction and their thermal and mechanical properties. Int J Rapid Solidification 1996;9(2):137–58.
[12] Inoue A, Katsuya A, Amiya K, Masumoto T. Preparation of amorphous Fe–Si–B and Co–Si–B alloy wires by a melt extraction method and their mechanical and magnetic properties. Mater Trans JIM 1995;36(7):802–9.
[13] Li JCM. Behavior and properties of shear bands. Polym Eng Sci 1984;24(10):750–60.
[14] Cao XG, Li JCM. Reverse shear of shear bands and annealing embrittlement in amorphous alloy. Acta Metall 1985;33(3):499–508.
[15] Grady DE, Kipp ME. The growth of unstable thermoplastic shear with application to steady-wave shock compression in solids. J Mech Phys Solids 1987;35(1):95–118.
[16] Wright TW. Scaling laws for adiabatic shear bands. Int J Solids Struct 1995;32(17/18):2745–50.
[17] Wright TW, Ockendon H. A scaling law for the effect of inertia on the formation of adiabatic shear bands. Int J Plast 1996;12(7):927–34.
[18] Molinari A. Collective behavior and spacing of adiabatic shear bands. J Mech Phys Solids 1997;45(9):1551–73.
[19] Nesterenko VF, Meyers MA, Wright TW. Self-organization in the initiation of adiabatic shear bands. Acta Mater 1998;46(1):327–40.
[20] Xue Q, Meyers MA, Nesterenko VF. Self-organziation of shear bands in Titanium and Ti–6Al–4V alloy. Acta Mater 2002;50:575–96.
[21] Conner RD, Johnson WL, Paton NE, Nix WD. Shear bands and cracking of metallic glass plates in bending. J Appl Phys 2003;94(2):904–11.
[22] Bruck HA, Christman T, Rosakis AJ, Johnson WL. Quasi-static constitutive behavior of $Zr_{41.3}Ti_{13.7}Ni_{10}Cu_{12.5}Be_{22.5}$ bulk amorphous alloys. Scr Metall Mater 1994;30(4):429–34.